

# High Resolution Templates for Step and Flash Imprint Lithography

D. J. Resnick<sup>a</sup>, W. J. Dauksher<sup>a</sup>, D. Mancini<sup>a</sup>, K. J. Nordquist<sup>a</sup>, E. Ainley<sup>a</sup>, K. Gehoski<sup>a</sup>, J. H. Baker<sup>a</sup>,  
T. C. Bailey<sup>b</sup>, B. J. Choi<sup>b</sup>, S. Johnson<sup>b</sup>, S. V. Sreenivasan<sup>b</sup>, J. G. Ekerdt<sup>b</sup>, and C. G. Willson<sup>b</sup>

<sup>a</sup>Physical Sciences Research Laboratories, Motorola Labs, Tempe, AZ 85284

<sup>b</sup>Texas Materials Institute, University of Texas at Austin, Austin, TX 78712

## ABSTRACT

Step and Flash Imprint Lithography (SFIL) is an attractive method for printing sub-100 nm geometries. Relative to other imprinting processes SFIL has the advantage that the template is transparent, thereby facilitating conventional overlay techniques. In addition, the imprint process is performed at low pressures and room temperature, minimizing magnification and distortion errors. The purpose of this work was to investigate alternative methods for defining high resolution SFIL templates and study the limits of the SFIL process. Two methods for fabricating templates were considered. The first method used a very thin (< 20 nm) layer of Cr as a hard mask. The second fabrication scheme attempts to address some of the weaknesses associated with a solid glass substrate. Because there is no conductive layer on the final template, SEM and defect inspection are compromised. By incorporating a conductive and transparent layer of indium tin oxide (ITO) on the glass substrate, charging is suppressed during SEM inspection, and the transparent nature of the final template is not affected. Using ZEP-520 as the electron beam imaging resist, features as small as 20 nm were resolved on the templates. Features were also successfully imprinted using both types of templates.

Keywords: Imprint, Lithography, Template, Step, and Flash

## 1. INTRODUCTION

Step and Flash Imprint Lithography (SFIL) is an attractive method for printing sub-100 nm geometries. Relative to other imprinting processes SFIL has the advantage that the template is transparent, thereby facilitating conventional overlay techniques. In addition, the imprint process is performed at low pressures and at room temperature,<sup>1</sup> which minimizes magnification and distortion errors.

Early template fabrication schemes started with a 6" × 6" × 0.25" conventional photomask plate and used established Cr and phase shift etch processes to define features in the glass substrate.<sup>2</sup> Although sub-100 nm geometries were demonstrated,<sup>3</sup> critical dimension (CD) losses during the etching of the thick Cr layer etch make the fabrication scheme impractical for 1X templates. It is not unusual, for example, to see etch biases as high as 100 nm.<sup>4</sup> The purpose of this work is to investigate alternative processes for defining features on an SFIL template.

The first method considered used a much thinner (< 20 nm) layer of Cr as a hard mask than is typically used in photomask production. Thinner layers still suppress charging during the e-beam exposure of the template, and have the advantage that CD losses encountered during the pattern transfer through the Cr are minimized. Because the etch selectivity of SiO<sub>2</sub> to Cr is better than 18:1 in a fluorine based process, a sub-20 nm Cr layer is also sufficient as a hard mask during the etching of the glass substrate. The second fabrication scheme attempts to address some of the weaknesses associated with a solid glass substrate. Because there is no conductive layer on the final template, SEM and defect inspection are compromised. By incorporating a conductive and transparent layer of indium tin oxide (ITO) on the glass substrate, charging is suppressed during SEM inspection, and the transparent nature of the final template is not affected.

## 2. EXPERIMENTAL DETAILS

In order to quickly establish baseline conditions, initial experiments were run on either 100 mm Pyrex 7740 wafers or 150 mm quartz wafers. Sumitomo NEB-22 negative resist was exposed on a Leica VB6 system operating at 100 kV. Features were exposed using a 5 nm address grid. The resist process used has been described previously.<sup>5</sup> Subsequent template development was done on 6" × 6" × 0.25" plates. Because it is difficult to uniformly heat a thick quartz substrate, NEB-22 resist was replaced with ZEP-520, a high resolution, non-chemically amplified positive electron resist available from the Zeon Corporation.<sup>6</sup> Cr was deposited in an MRC 603 D.C. magnetron load locked sputtering system. A 1200 W, 35 mTorr process run in a single pass mode was employed. The first test samples of ITO were supplied by Silicon Quest, and were D.C. sputtered at a power of 1 kW in 100% Ar at a pressure of 8 mTorr. Subsequent development was done internally in a customized RF sputter system operating at a power of 100 W and an Ar/O<sub>2</sub> pressure of 6 mTorr. The films were then annealed at a temperature exceeding 250 °C for one hour in order to further improve optical transmission and conductivity, PECVD oxide was deposited in a Novellus Concept 1 system at a temperature of 250 °C. All pattern transfer experiments were performed in a Unaxis VLR system. A chlorine and oxygen mixture was used to etch the Cr films.<sup>7</sup> A CHF<sub>3</sub> based etch was used to pattern transfer into the SiO<sub>2</sub> materials.

CD measurements and top down micrographs were taken with a Hitachi S7800 CD-SEM equipped with a cold cathode source and an automated pattern recognition system. The repeatability of the CD-SEM is 3.5 nm (3 $\sigma$ ) for line measurements and 1.4 nm (3 $\sigma$ ) for pitch. Cross-sectioned images were obtained with a Hitachi S4500 SEM operating at 5 kV.

## 3. THIN CR PROCESS

### 3.1 Results on quartz wafers

To minimize CD loss Cr film, layers as thin as 10 nm were deposited on 150 mm quartz wafers. In earlier work, 180 nm thick NEB-22 resist was exposed on the VB6 and served as the hard mask for the pattern transfer of the Cr.<sup>8</sup> The Cr was then used as the hard mask for the transfer of the image into the quartz. Following the quartz etch, the remaining resist and Cr were stripped away, thereby producing a final template. Typical etch depths into the quartz were 100 nm. A schematic of the process is depicted in Figure 1.

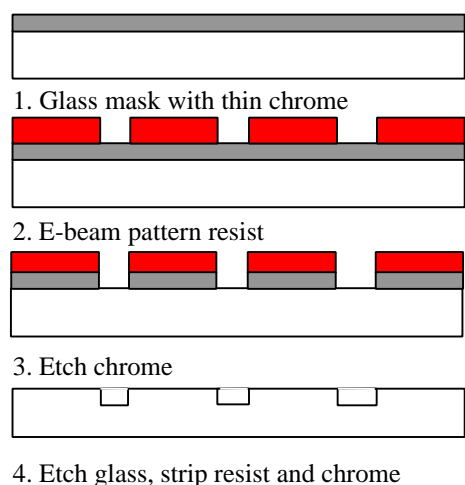


Figure 1. Schematic of a Cr based template.

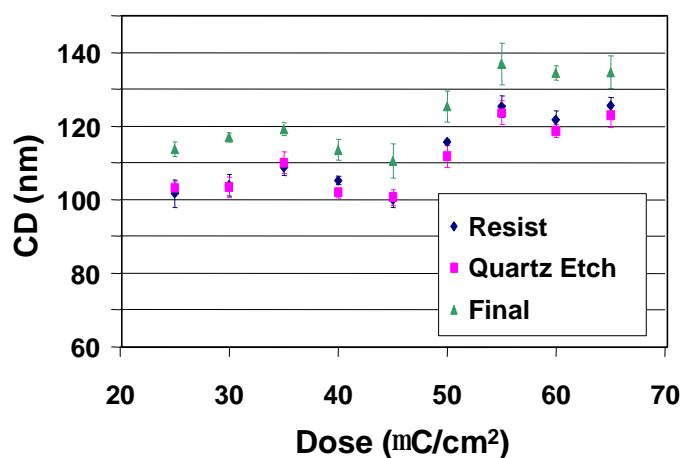


Figure 2. CD vs. exposure dose, before and after process pattern transfer.

Figure 2 depicts the change in CD for 100 nm lines as the template was processed. No discernable shift in CD was detected after the etching of both the Cr and quartz. After stripping the resist and Cr, the template was coated with a 5 nm blanket film of Cr (to avoid charging in the SEM) and measured again. A 10 nm shift was observed, and is most likely a consequence of the blanket charge reduction layer. Figure 3 depicts SEM images of 35 nm trenches and 50 nm lines in the final template.

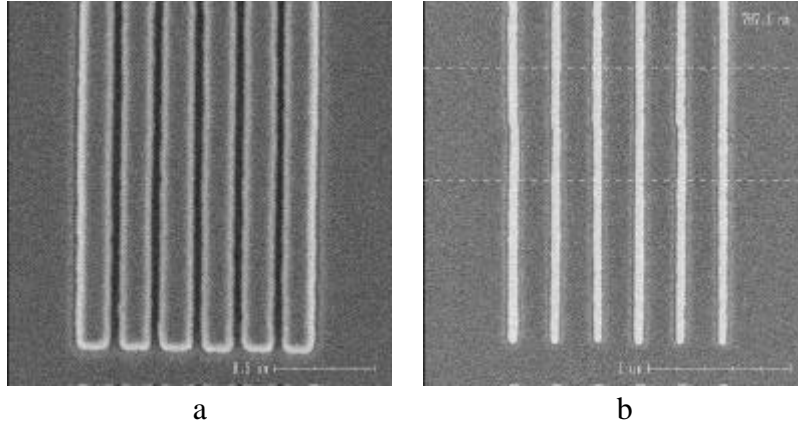


Figure 3. 35 nm trenches and 50 nm lines defined in an SFIL quartz wafer.

### 3.2 Results on 6025 plates

The current SFIL template form factor is  $1.0'' \times 1.0'' \times 0.25''$ . In order to print with templates fabricated from wafers, as described above, it was necessary to cut a section from the wafer and epoxy the sample to a quartz blank. It is not possible to maintain template surface flatness with this procedure, and several fringes were easily observed in the etch barrier after printing, indicating a non-uniform imprint field. To eliminate this effect, the processing migrated to a conventional  $6'' \times 6'' \times 0.25''$  quartz plate.

The most pressing issue associated with processing on quartz plates is the resist process. Because the quartz is a poor thermal conductor, it is difficult to obtain good temperature uniformity across the plate. This is particularly concerning for a chemically amplified resist such as NEB-22, since CD control is sensitive to the post exposure bake process. A CD shift of  $7 \text{ nm}/^\circ\text{C}$  is typical. To avoid this problem and attempt to obtain smaller features on the finished template, and to minimize line edge roughness, a switch was made to ZEP-520.

ZEP-520 is a positive chain-scission-type resist consisting of copolymers of  $\alpha$ -chloromethacrylate and  $\alpha$ -methylstyrene. A variety of developers have successfully been used, and excellent resolution has previously been demonstrated.<sup>6</sup> In order to obtain good resolution and minimize swelling, a 50/50 mix of MIBK and IPA was chosen for this study. Typical exposure doses for a 100 kV system range between  $500$  and  $1000 \mu\text{C}/\text{cm}^2$ . Examples of 30 and 40 nm features exposed in 180 nm of ZEP-520 are depicted in Figure 4.

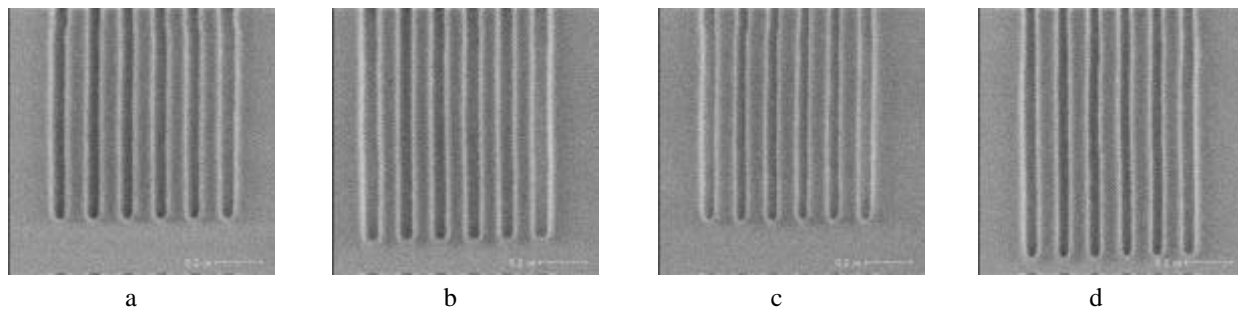


Figure 4. The first two SEMs depict 40 nm trenches exposed at  $700$  and  $800 \mu\text{C}/\text{cm}^2$ , respectively. The final two SEMs depict 30 nm trenches exposed at  $700$  and  $800 \mu\text{C}/\text{cm}^2$ . The lines separating the trenches were held constant at 100 nm.

Resist latitude is depicted in Figure 5. Below  $600 \mu\text{C}/\text{cm}^2$ , the smaller features were not completely resolved. At  $600 \mu\text{C}/\text{cm}^2$ , measured CDs exceeded the coded values by approximately 10 nm.

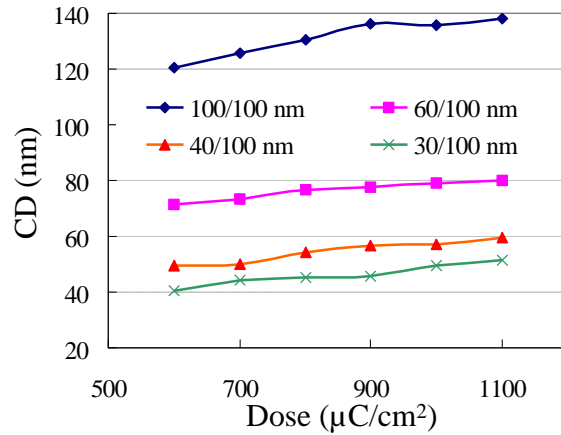


Figure 5. Feature size as a function of exposure dose for 180 nm thick ZEP-520 resist.

The template exposure and pattern transfer process consisted of exposure and development of the ZEP-520, followed by an oxygen descum, Cr etch, resist strip, quartz etch and a Cr wet etch. It is interesting to note that it was necessary to remove the resist prior to the quartz etch. If left in place during the  $\text{CHF}_3$  based quartz etch, the amount of polymer deposited during the etch process is substantial enough to impact the fidelity of the quartz features. Additional amounts of oxygen may be necessary to minimize polymer formation. The process sequence for several feature sizes is depicted below. The exposure dose for each case was  $600 \mu\text{C}/\text{cm}^2$ . Etch depth of the quartz was approximately 120 nm.

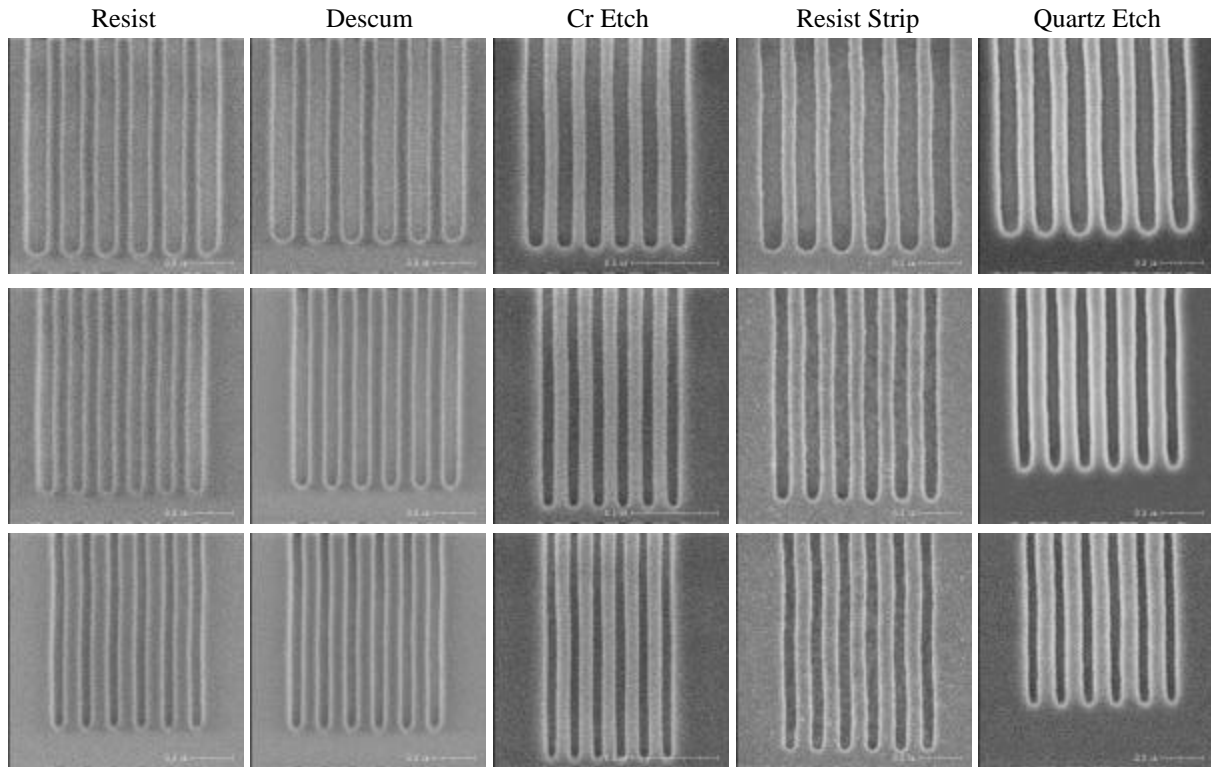


Figure 6. Pattern transfer sequence for 60 nm (row 1), 40 nm (row 2), and 30 nm (row 3) trenches. Lines between the trenches are 100 nm.

At higher exposure doses, the 20 nm features were also resolved, although defects were observed in the final quartz etch. Resolution of these features was surprising, since the aspect ratio of the resist feature was approximately 9:1. An example of 20 nm trenches is depicted in Figure 7.

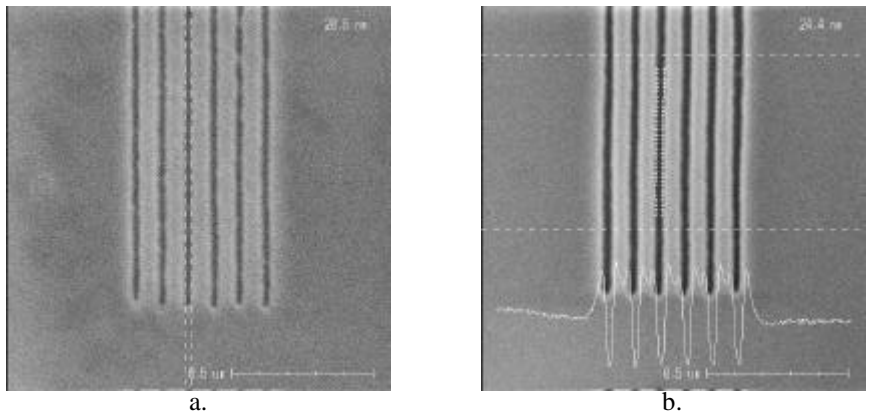


Figure 7. 20 nm trenches etched in the quartz template. The electron beam exposure doses for pictures a. and b. were 600 and 800  $\mu\text{C}/\text{cm}^2$ , respectively. Measured trench size ranged from 20 to 25 nm.

It is apparent that there is minimal change in CD throughout the entire pattern transfer process. We attribute this to the good etch resistance of the ZEP-520, the reduced thickness of the Cr hardmask, and the anisotropic nature of the quartz etch. The actual breakdown of each process step is shown in Table 1. The deviations from the initial resist CD for the 100, 60, 40 and 30 nm features are shown for each pattern transfer step. The final CD for each feature size is smaller than the resist CD on average by about 5 nm. It is also observed that the difference is largest for the smallest features measured. As an example, the coded 30 nm trenches were originally measuring 41 nm. Final feature size after the quartz etch was 33 nm. It is not clear, however, whether this behavior is related to processing or measurement, or both. More data and cross-sections SEMs will be required to better understand this trend.

*L/S Patt	Process	Resist Descum	?	150Å Cr Etch	?	Resist Strip	?	Quartz Etch	?	Cr Strip (Final)	?
100/100		122	1.7	122.5	2.2	129.5	9.2	119.2	-1.1	118.5	-1.8
60/100		72.8	-2	71.7	.4	78.2	6.9	67.4	-3.9	66.4	-4.9
40/100		50.9	1.6	45.7	-3.6	51.9	2.6	40.2	-9.1	43.2	-6.1
30/100		40.1	-6	38.2	-2.5	38.9	-1.8	31.6	-9.1	32.9	-7.8

\* L/S: Line/Space pattern, all values in nm

Table 1. Measured feature size for each pattern transfer step. Final feature sizes are somewhat smaller than the measured resist feature.

### 3.3 Printing Results

A 248 nm Ultratech stepper has been converted to function as an imprint step and repeat tool, and has been detailed previously.<sup>3</sup> Templates and wafers were loaded and unloaded manually. Printing operations, including x-y positioning of the wafer, dispensing etch barrier liquid, z-translation of the template to close the gap between the template and wafer, UV curing of etch barrier, and controlled separation are all automated and controlled with a LabVIEW interface.<sup>9</sup> The system is currently configured to handle 1"  $\times$  1"  $\times$  0.25" templates. A custom saw process was used to cut the original photomask plate into templates compatible with the printing system.

The SFIL etch barrier solution is a solventless, low viscosity, UV curable solution containing a combination of organic and organosilicon acrylate monomers, and a photoinitiator. The formulation used in these experiments consisted of 96% (w/w) 1,3-bis(3-methacryloxypropyl)tetramethyldisiloxane (Gelestand 4% 2-hydroxy-2-methyl-1-phenyl-propan-1-one (Ciba). The template was imprinted on approximately 100 nl of this solution, and the stack was illuminated through the template backside using a 500 W Oriel Hg arc lamp. After the completion of the photocuring process, the template was withdrawn from the substrate.

Imprinting results are shown in Figure 8a, which depicts semi-dense lines with dimensions of 60 nm, 40 nm, 30 nm and 20 nm. The break in the 20 nm lines is a consequence of both the fidelity of the template and the high aspect ratio of the features. An example of the repeatability of the SFIL process is shown in Figure 8b. Depicted are 30 nm lines resulting from four different imprints. A very small butting error (on the order of a few nanometers) is visible in the left most line and is observed in each imprint.

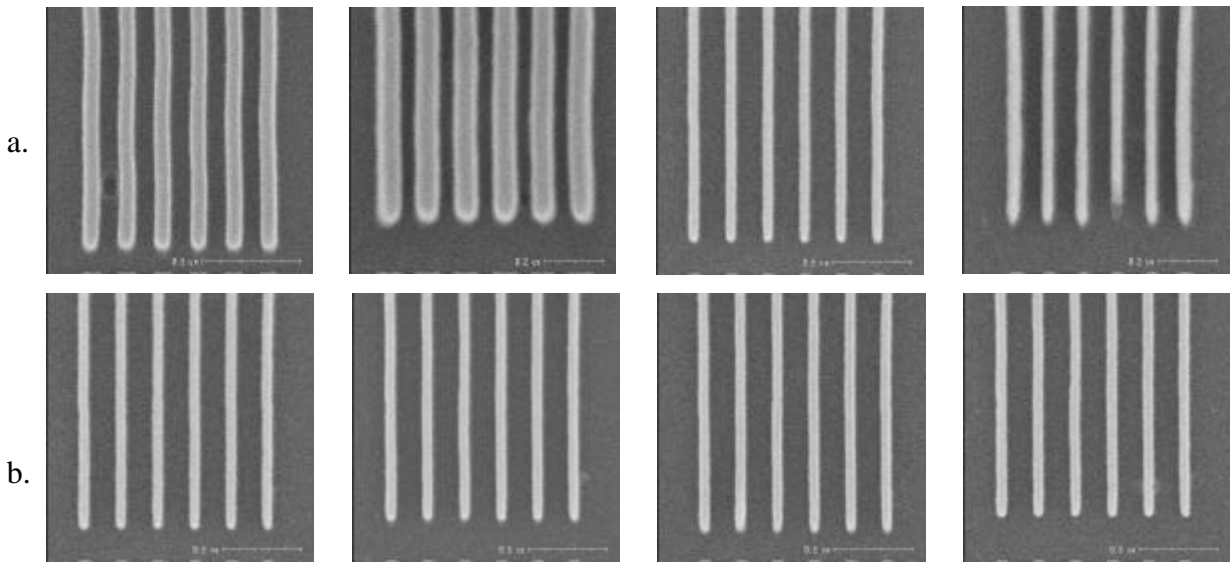


Figure 8. a.) Semi-dense 60, 40, 30 and 20 nm lines. b.) 30 nm printed lines from four different die.

Cross-section SEM examples are shown in Figure 9. Again, pattern fidelity is excellent for features as small as 30 nm. The 20 nm lines, although resolved, show evidence of collapse, a consequence of the 6:1 aspect ratio of the trenches present in the template.

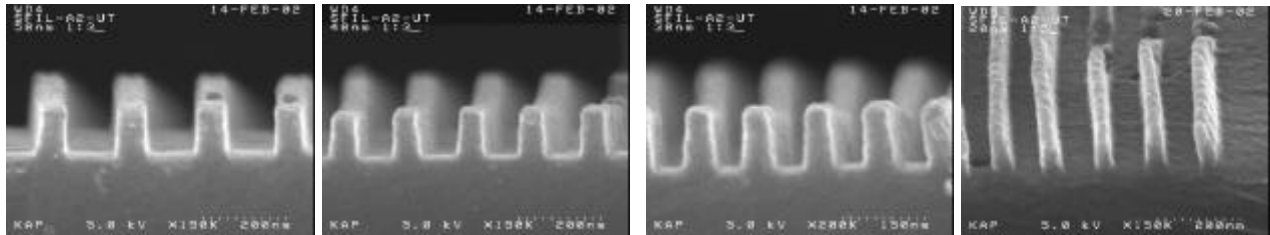


Figure 9. Cross-section SEM images for (left to right) 50, 40, 30 and 20 nm semi-dense lines.

## 4. ITO/OXIDE TEMPLATES

### 4.1 ITO/Oxide Pattern transfer process

Although it is possible to resolve very small features using the process described in Section 3, the final templates have some potentially serious limitations. The height of a feature on a printed wafer becomes a function of the quartz etch. It is well known that microloading effects during an etch process cause variations in etch rate that are a function of feature size. In addition, because the previous process produces a template with features defined directly in the quartz, it is difficult to use electron beam techniques to inspect the final template. It is also difficult to optically measure image placement with this format. By incorporating a transparent conducting oxide, such as indium tin oxide (ITO) into the template, all the problems described above can be addressed. The process necessary to produce this type of template is depicted schematically in Figure 10.

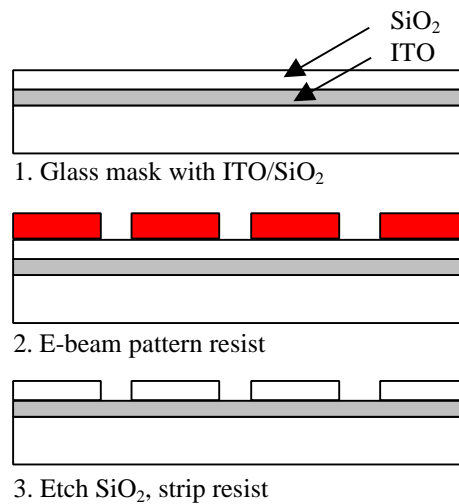


Figure 10. Schematic of a pattern transfer processing for a template including a transparent conducting oxide.

A sputter deposited ITO film is placed directly on the quartz plate, followed by a PECVD SiO<sub>2</sub> film. The thickness of the SiO<sub>2</sub>, which determined imprinted feature height, is determined by the aspect ratio required during SFIL imprinting and subsequent etching. The SiO<sub>2</sub> is then coated with an e-beam resist. The resist is patterned and subsequently used as an etch mask for the SiO<sub>2</sub> pattern transfer. Because fluorine forms no volatile products with either indium or tin, the ITO serves as an excellent etch stop. The ITO remains part of the template and serves as a contrast material for inspection.

Previous work has demonstrated the viability of the pattern transfer process.<sup>10</sup> Examples of 70 nm and 100 nm images on a template, using NEB-22 as the electron beam imaging resist are depicted in Figure 11.

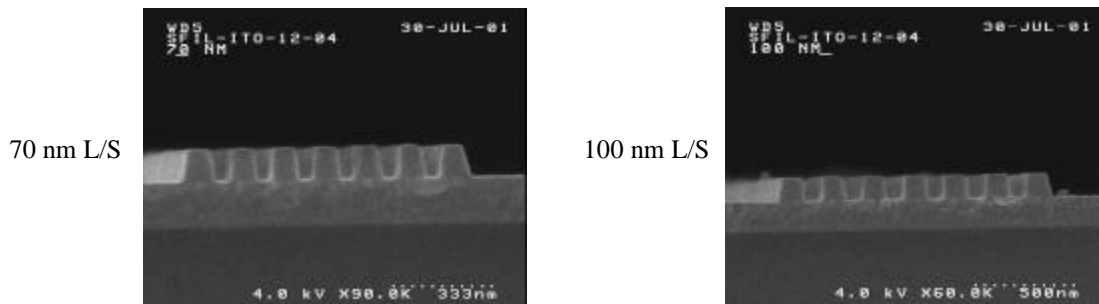


Figure 11. Cross-section SEM images of dense 70 nm (a) and 100 nm (b) lines.

The transparent conducting oxide, ITO in this case, must satisfy a large number of criteria to be successfully implemented. The material must be transparent at 365 nm (in order to allow polymerization the etch barrier layer during the SFIL imprinting process), but be reflective enough at 780 nm to allow the laser height sensor system of the VB6 to locate the template surface during template exposure. Resistivity must be low enough to allow e-beam writing and template inspection without charging. Additionally, the ITO must have minimal surface roughness, possess sufficient adhesion to SiO<sub>2</sub> in order to withstand the imprint process, and be compatible with the release layer that is applied to the template prior to imprinting. Finally, stress in both the ITO and SiO<sub>2</sub> films must be minimized in order to avoid image placement errors and deviations in template flatness.

ITO samples were initially obtained from Silicon Quest. A parallel effort was also started in-house to develop an ITO deposition process. By optimizing the deposition parameters, it is now possible to obtain high conductivity films with transmission (at 365 nm) above 70% and rms surface roughness less than 0.5 nm. This result is particularly important, since excess surface roughness is imparted to the etch barrier and also serves to create false defects during the template defect inspection process. An AFM image of a typical ITO film is shown in Figure 12.

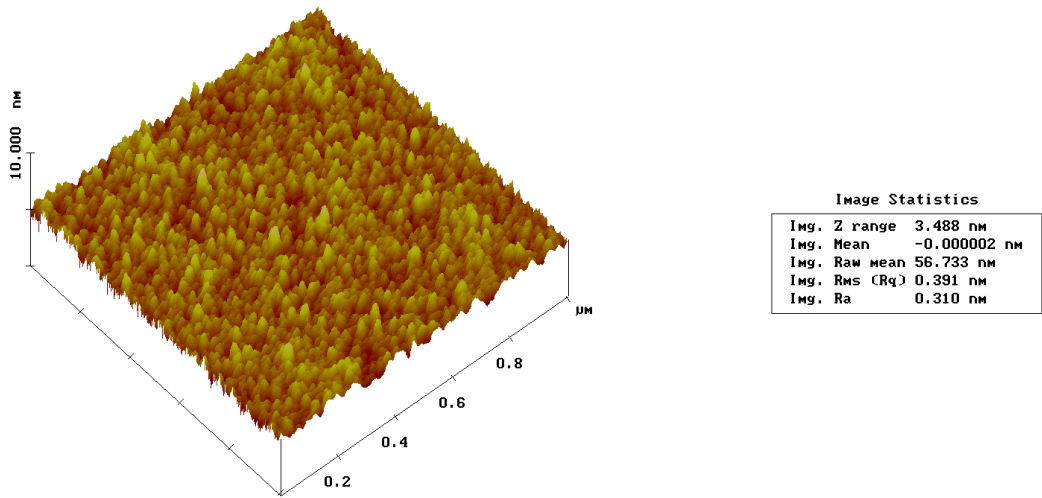


Figure 12. AFM image of a sputter deposited ITO film. RMS surface roughness is less than 0.40 nm. Peak-to-valley range is less than 4 nm.

Previous work has also shown the ITO film to be sufficiently conductive. Dense 50 nm resist lines were clearly resolved and clean SEM images were easily obtained in the finished template. Future work will focus on transferring the process to quartz plates along with performing more rigorous experiments to determine compatibility with existing metrology systems.

### 4.3 Printing Results

Printed images were obtained by cutting a small section from the quartz wafer and epoxying the sample to a blank template. This process introduces exposure uniformity and mask flatness errors, making reproducible results difficult to obtain. Initial imprints yielded features as small as 65 nm, as shown in Figure 13. After transferring the process to quartz plates and implementing the ZEP-520 process, we expect to obtain improved resolution and good uniformity across a die and from die to die.



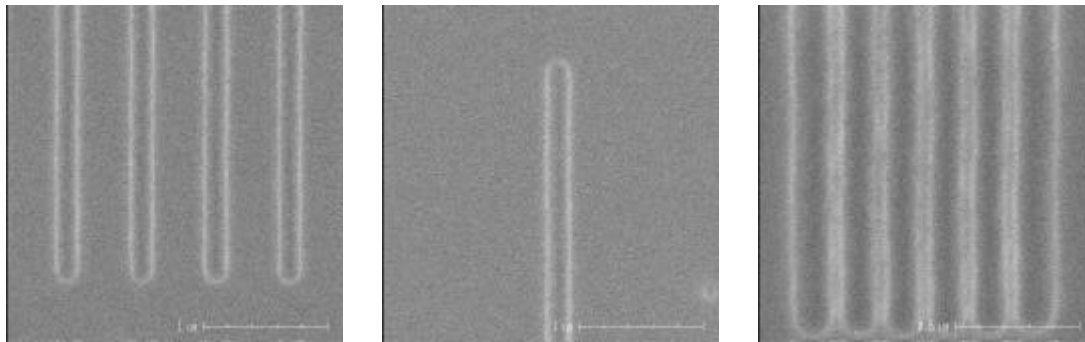


Figure 13. SEM images of sub-100 nm features obtained using an ITO-based template. Even at critical dimensions of 65 nm (right), the etch barrier maintains good fidelity.

## 5. CONCLUSIONS

Two different methods have been used to produce high-resolution templates suitable for Step and Flash Imprint Lithography. Template features as small as 20 nm were obtained by switching to ZEP-520 resist and using a very thin Cr film as the hardmask. The smallest features in the template were also successfully printed. Proof of concept for employing a transparent conductive oxide as an etch stop has also been demonstrated. Printed 65 nm features were resolved. It is expected that better resolution will be obtained when the ITO/SiO<sub>2</sub> process is transferred to quartz plates. Future work will focus on further optimization of the ITO films. New work will also be started to examine the issues associated with fabricating simple devices.

## ACKNOWLEDGEMENTS

The authors gratefully acknowledge Steve Smith, Dolph Rios, Eric Newlin, David Standfast, and Mario Meissl for their process help. We would also like to thank Lyndi Noetzel, Lester Casoose, Kathy Palmer, Diane Convey, Andy Hooper and Alec Talin for their characterization work. Finally, we thank Laura Siragusa and Jim Prendergast for their support. This work was partially funded by DARPA (BAA 01-08/01-8964 and MDA972-97-1-0010) and SRC (96-LC-460).

## REFERENCES

1. T. Bailey, B. J. Choi, M. Colburn, M. Meissl, S. Shaya, J. G. Ekerdt, S. V. Sreenivasan, and C. G. Willson, *J. Vac. Sci. Technol. B* 18(6), 3572 (2000).
2. M. Colburn, S. Johnson, M. Stewart, S. Damle, T. Bailey, B. Choi, M. Wedlake, T. Michaelson, S. V. Sreenivasan, J. Ekerdt, and C. G. Willson, *Proc. SPIE, Emerging Lithographic Technologies III*, 379 (1999).
3. M. Colburn, T. Bailey, B. J. Choi, J. G. Ekerdt, S. V. Sreenivasan, *Solid State Technology*, 67, June 2001.
4. C. Constantine, R. Westerman, and J. Plumhoff, *Proc. SPIE* 3748, 153 (1999).
5. K. H. Smith, J. R. Wasson, P. J. S. Mangat, W. J. Dauksher and D. J. Resnick, to be published in *J. Vac. Sci. Technol. B*. Nov/Dec 2001.
6. H. Namatsu, M. Nagase, K. Kurihara, K. Iwadate, T. Furuta, and K. Murase, *Jpn. J. Appl. Phys.* 34, 6940 (1995).
7. K. H. Smith, J. R. Wasson, P. J. S. Mangat, W. J. Dauksher, D. J. Resnick, *J. Vac. Sci. Technol. B* 19(6), 2906 (2001)
8. T. C. Bailey, D. J. Resnick, D. Mancini, K. J. Nordquist, W. J. Dauksher, E. Ainley, A. Talin, K. Gehoski, J. H. Baker, B. J. Choi, S. Johnson, M. Colburn, M. Meissl, S. V. Sreenivasan, J. G. Ekerdt, and C. G. Willson, to be published in *Microelectronic Engineering* 2002.
9. B.J. Choi, S. Johnson, M. Colburn, S.V. Sreenivasan, C.G. Willson., *Precision Eng.*, 25(3), 192 (2001).
10. D. J. Resnick, T. C. Bailey, D. Mancini, K. J. Nordquist, W. J. Dauksher, E. Ainley, A. Talin, K. Gehoski, J. H. Baker, B. J. Choi, S. Johnson, M. Colburn, M. Meissl, S. V. Sreenivasan, J. G. Ekerdt, and C. G. Willson, to be published in the *SPIE Proc. on Nanotechnology*, 2001.